



Contents lists available at ScienceDirect

Bioorganic & Medicinal Chemistry

journal homepage: www.elsevier.com/locate/bmc

Synthesis and evaluation of 2,5 and 2,6 pyridine-based CXCR4 inhibitors

Theresa Gaines^a, Davita Camp^a, Renren Bai^b, Zhongxing Liang^{b,c}, Younghyun Yoon^c, Hyunsuk Shim^{a,b}, Suazette Reid Mooring^{a,*}

^a Department of Chemistry, Georgia State University, Atlanta, GA 30303, USA

^b Department of Radiology and Imaging Science, Emory University School of Medicine, Atlanta, GA 30322, USA

^c Winship Cancer Institute, Emory University, Atlanta, GA 30322, USA

ARTICLE INFO

Article history:

Received 8 June 2016

Revised 8 August 2016

Accepted 12 August 2016

Available online xxxxx

Keywords:

Pyridine

CXCR4 inhibitor

Matrigel invasion

Binding affinity

Cancer metastasis

Anti-inflammatory

ABSTRACT

Targeting the interaction between G-Protein Coupled Receptor, CXCR4, and its natural ligand CXCL12 is a leading strategy to mitigate cancer metastasis and reduce inflammation. Several pyridine-based compounds modeled after known small molecule CXCR4 antagonists, AMD3100 and WZ811, were synthesized. Nine hit compounds were identified. These compounds showed lower binding concentrations than AMD3100 (1000 nM) and six of the nine compounds had an effective concentration (EC) less than or equal to WZ811 (10 nM). Two of the hit compounds (**2g** and **2w**) inhibited invasion of metastatic cells at a higher rate than AMD3100 (62%). Compounds **2g** and **2w** also inhibit inflammation in the same range as WZ811 in the paw edema test at 40% reduction in inflammation. These preliminary results are the promising foundation of a new class of pyridine-based CXCR4 antagonists.

© 2016 Elsevier Ltd. All rights reserved.

1. Introduction

Cancer is a dreadful diagnosis with the potential for a bitter prognosis. The five-year survival rate for cancer drops drastically when the cancer reaches stage IV.^{1,2} Metastasis, the ability for cancer cells to migrate to distant places in the body, is the only factor that defines cancer as stage IV.¹ Many metastatic cancers exhibit an over-expression of the chemokine receptor CXCR4. CXCR4 is a seven trans-membrane protein receptor that binds to the chemokine ligand, CXCL12.³ The interaction between CXCL12 and CXCR4 triggers downstream pathways that can induce inflammation,⁴ mobilize stem cells,⁵ and promote cancer cell metastasis.⁵ Since the CXCR4–CXCL12 axis plays such an important role in these disease related pathways, blocking this interaction has become a leading strategy in an attempt to reduce the progression of cancer and other inflammatory conditions.⁷ Several small molecule antagonists have had success in blocking this interaction and have been shown to inhibit cancer metastasis, and have anti-inflammatory activity.^{8–11} This work centers on the synthesis of pyridine derivatives as small molecule antagonists to block the interaction between CXCR4 and CXCL12.¹²

One of the first small molecule inhibitors of CXCR4 to show promise was AMD3100.¹³ The precursor to this compound was discovered as an impurity that showed anti-HIV activity by blocking CXCR4, which is one of the receptors HIV-1 uses to enter the cell. This impurity was composed of two cyclam rings connected together by an aliphatic chain. Replacing the aliphatic linker with a benzene ring increased the potency of the compound—resulting in AMD3100 (Fig. 1).¹⁴ Other non-aromatic rings derivatives of AMD3100 were synthesized and tested for activity, but only the compounds featuring benzene rings were active.¹⁵

AMD3100 was the first FDA approved CXCR4 antagonist; however, even though the initial purpose for this compound was to block HIV-1 entry into the cells, this drug was not approved for this purpose.¹⁶ In addition to poor oral bioavailability,^{17,18} AMD3100 is cardiotoxic.^{17,19} The FDA approved AMD3100 for limited use in patients with multiple myeloma in order to mobilize and harvest stem cells.^{14,20,21}

It was speculated that the toxicity and poor oral bioavailability of AMD3100 stemmed from the bicyclam rings. In order to verify this, new analogues were design and synthesized in which the bicyclams rings were replaced. These studies led to the synthesis of a potent *p*-xylyl-enediamines derivate, WZ811 (Fig. 1).²² There are several other categories of CXCR4 antagonists including: cyclic pentapeptide-based antagonists, indole based antagonists, and

* Corresponding author.

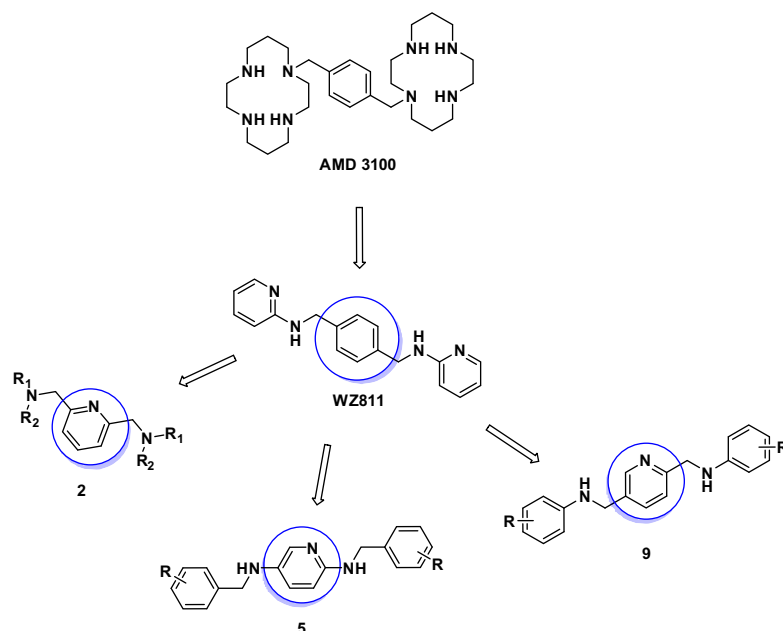


Figure 1. Progression from AMD3100 to WZ811 to the pyridine-based compounds that have been synthesized in this work.

tetrahydroquinoline-based antagonists.²³ Various substituents and side chains have been analyzed in the *p*-xylyl-enediamine class of compounds and have been screened for CXCR4 activity. The cyclams and bicyclams are among the most studied in this group;²² however, there have not been any structure–activity relationship (SAR) studies in which the central phenyl ring has been altered. Many of the *p*-xylyl-enediamine compounds have shown CXCR4 activity but very few have gone on to clinical trials primarily due to toxicity or bioavailability issues.²³

Pyridine rings are common motifs in compounds for therapeutic purposes (Fig. 1).²⁴ Pyridine rings have a lower log*P* value than benzene rings therefore it is possible this new class of pyridine based compounds will yield potent antagonists with better pharmacological properties such as oral bioavailability and pharmacokinetics.²⁵ In this present study, a pyridine ring replaces the central phenyl ring. Two classes of pyridine compounds were explored, 2,5 substituted, and 2,6 diamino substituted pyridines (Fig. 1).

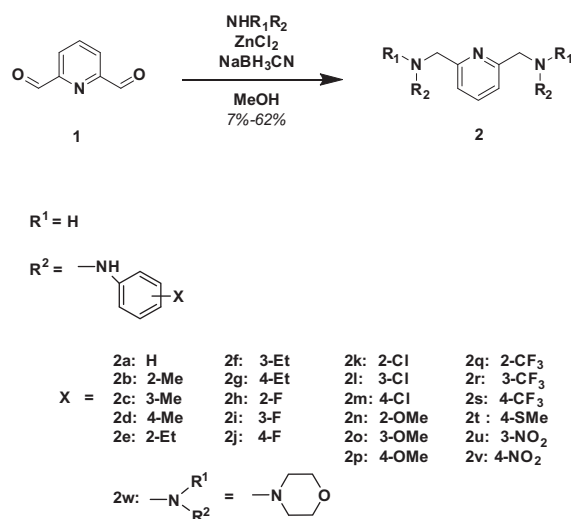
2. Results and discussion

2.1. Chemistry

The 2,6-pyridine analogues (**2a–w**) were synthesized via a reductive amination reaction between 2,6-pyridinedicarbaldehyde (**1**) and a substituted amine. The 2,5-diaminopyridine analogues (**5a–d**) were also prepared via reductive amination using 2,5-diaminopyridine (**3**) and a substituted benzaldehyde (**4**). Similarly, the 2,5-bis(anilinomethyl)pyridine analogues (**9a–c**) were synthesized by reductive amination of 2,5-pyridinedicarboxaldehyde (**8**) and a substituted amine. Compound **8** was synthesized from the reduction of 2,5-dimethylcarboxylatepyridine (**6**) with NaBH₄ followed by oxidation of the resulting di-alcohol **7** with MnO₂ under reflux conditions. The synthesis routes and reagents used are outlined in Schemes 1–3.

2.2. Binding assay

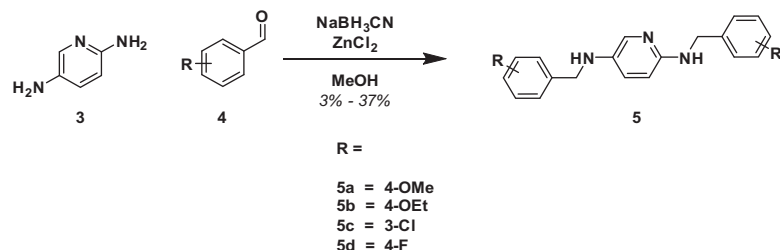
The derivatives were tested in a semi-quantitative binding affinity assay. It is important to emphasize that this assay is used



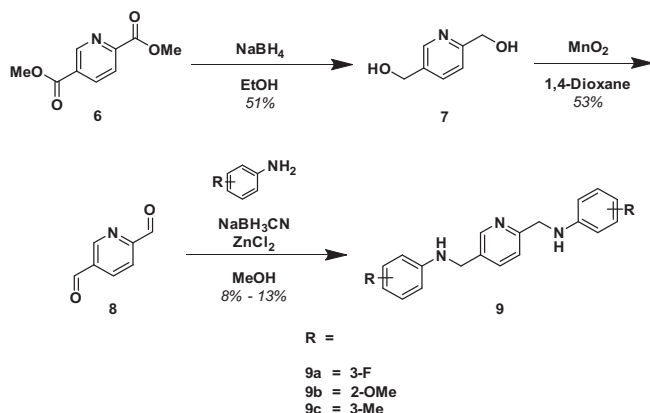
Scheme 1. Synthesis of 2,6-pyridine derivatives.

as a preliminary screen for potential CXCR4 antagonists that will warrant further testing. The MDA-MB-231 breast cancer cells are incubated with the compounds at 1 nM, 10 nM, 100 nM and 1000 nM concentrations. Next, the cells are incubated with a biotinylated peptide, TN14003 (a known CXCR4 inhibitor), followed by streptavidin-rhodamine. The fluorescence of the cells is then measured to obtain effective concentration (EC) is obtained. EC is the lowest concentration of the compound where there is a significant reduction in fluorescence observed compared to the positive control as shown in Figure 2. All compounds synthesized were screened using this binding assay. Compounds that scored at 100 nM and below were then subjected to the Matrigel invasion assay. In total, 14 of the 42 compound synthesized scored at 100 nM or lower.

Out of all the compounds tested, there were a few categories of compounds that performed well in the binding assay. R groups with a terminal ethyl side chain in either the ortho (**2e**) or para



Scheme 2. Synthesis of 2,5-diaminopyridine derivatives.



Scheme 3. Synthesis of 2,5-bispyridineanilino derivatives.

position (**2g**) exhibited promising results in the binding assay. It didn't matter if the chain was an ethyl (**2e** and **2g**) or an ethoxy (**5b**); however, positioning mattered. When the ethyl group was in the meta position (**2f**), activity dropped off. Similarly, groups with terminal methyl side chains exhibited promising results when in the meta position—this includes methyl groups (**2c** and **9c**) and methoxy groups (**2o**). Halogens only showed activity when in the meta position of the aniline on the 2,6-pyridine derivatives (**2f** and **2i**). The trifluoromethyl aniline compound also performed well in the binding assay but only in the para position (**2s**). Lastly, the morpholino compound (**2w**) exhibited promising results. It is possible that the lone pairs on the oxygen of the morpholine provide some sort of interaction in the active site of CXCR4.

2.3. Matrigel invasion assay

The Matrigel invasion assay is used as a functional assay to probe if the synthesized analogues can block CXCR4/CXCL12 mediated chemotaxis and invasion. This assay uses a special two chambered apparatus. MDA-MB-231 cells that have been incubated in 100 nM concentrations of the analogues are placed in the top chamber and CXCL12 is placed in the bottom chamber as a chemoattractant. The partition between the two chambers is a Matrigel matrix that the MDA-MB-231 cells can pass through. The measurement gained in this assay is a percentage of inhibition of chemotaxis. When the assay is complete, the number of cells that migrated through the matrix is counted. The percent inhibition is the percentage of cells that were prevented from migrating compared to the negative control. The stronger the inhibitor, the fewer cells that pass through the membrane. The results for this assay have been consolidated with the results from the binding assay in Table 1.

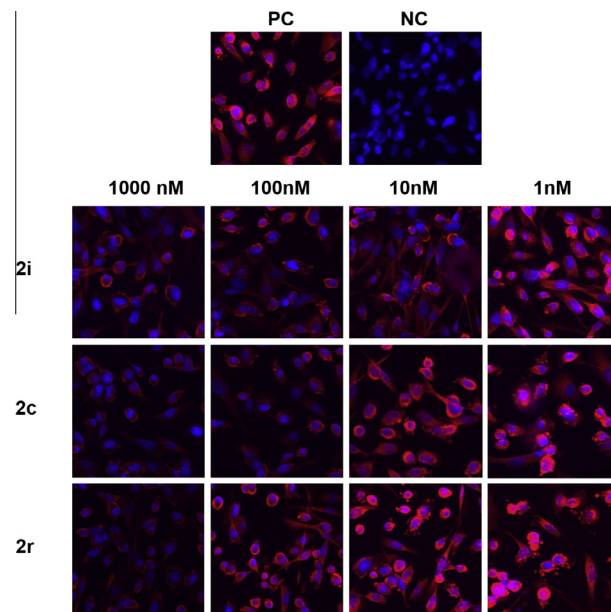
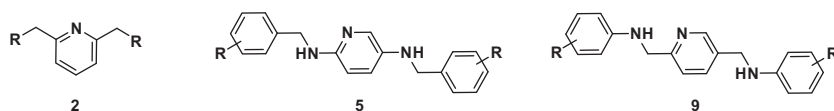


Figure 2. Reduction of inflammation observed for selected derivatives. **2i** had an EC of 10 nM. **2c** had an EC of 100 nM and **2r** had an EC of 1000 nM.

Only the compounds that showed promise in the binding assay ($EC \leq 100$ nM) were tested in the Matrigel invasion assay. The two compounds used as benchmarks were AMD3100 and WZ811. An invasion inhibition above 35% was favorable. Nine compounds subjected to this assay showed favorable results; however, there are no strong trends. The compounds that have shown favorable inhibition have substituents in the ortho, meta and para positions. Several compounds had test results on par with AMD3100 (1000 nM and 62%)^{26,27} and WZ811 (10 nM and 90%).²² Eight of the nine compounds inhibited over 50% of the migrating cell. None of the compounds synthesized inhibited cell migration above 70%; however, since CXCR4 is a necessary receptor for physiological functions, complete inhibition of invasion would make these compounds unsuitable for medicinal applications. The nine compounds that inhibited migration more than 35% were then tested in the carrageenan paw edema test.

Together, these assays give information about which of our pyridine analogues bind to CXCR4, at which concentrations and which ones can prevent chemotaxis from occurring in vitro. From these results several hit compounds (Table 2) were identified. Hit compounds were identified as compounds that scored at 100 nM or lower in the binding assay, and had a 35% or higher score for the invasion assay. Out of these hit compounds, only the 2,6-pyridine compounds were selected for further testing using a carrageenan induced paw edema test.

Table 1
Binding and invasion assay results for all analogues synthesized

Compd	R Group	EC (nM)	Invasion ^a (%)	Compd	R Group	EC (nM)	Invasion ^a (%)
2a	Aniline	100	<1	2p	4-Ome aniline	100	5
2b	2-Me aniline	>1000	—	2q	2-CF ₃ aniline	>1000	—
2c	3-Me aniline	100	60	2r	3-CF ₃ aniline	1000	15
2d	4-Me aniline	1000	—	2s	4-CF ₃ aniline	1	52
2e	2-Et aniline	1	59	2t	4-SMe aniline	>1000	—
2f	3-Et aniline	1000	—	2u	3-NO ₂ aniline	>1000	—
2g	4-Et aniline	—	64	2v	4-NO ₂ aniline	>1000	—
2h	2-F aniline	1000	—	2w	Morpholine	10	63
2i	3-F aniline	10	50	5a	4-Ome	1000	—
2j	4-F aniline	100	5	5b	4-OEt	100	60
2k	2-Cl aniline	>1000	—	5c	3-Cl	1000	—
2l	3-Cl aniline	100	34	5d	4-F	>1000	—
2m	4-Cl aniline	100	21	9a	3-F	1000	—
2n	2-OMe aniline	1000	0	9b	2-OMe	100	<5
2o	3-OMe aniline	100	37	9c	3-Me	1	58
AMD3100 ^{26,27}	—	1000	62				
WZ811 ²²	—	10	90				

^a The invasion assay concentration used for all compounds tested was 100 nM.

Table 2
Assay and test results for hit compounds

Compd	EC (nM)	Invasion ^a (%)	Carageenan ^b (%)
2c	100	60	20.2
2e	1	59	18.1
2g	1	64	42.0
2i	10	50	20.3
2o	100	37	20.1
2s	1	52	20.3
2w	10	63	39.1
5b	100	60	—
9c	1	58	—
AMD3100 ^{26,27}	1000	62	—
WZ811 ²²	10	90	40

^a The concentration used in the invasion assay was 100 nM.

^b Mice were dosed used 10 mg of compound for every kg the mouse weighed.

2.4. In vivo carrageenan suppression

The mouse paw edema model is used as a proof-of-concept test.^{22,26} If these analogues are able to disrupt the CXCR4–CXCL12 interaction, then it also has an effect on inflammation. If inflammation were to be induced in the presence of these compounds, a reduction in said inflammation would be observed for potent CXCR4 antagonists. All compounds that performed well in both the binding assay and Matrigel invasion assay were submitted for the paw edema test. This test is also a way to gain insight into the toxicity of our compounds. None of the mice that were given the synthesized analogues died before the completion of this test.

Out of the nine compounds tested, two showed promising results. Compounds **2g** (4-methyl aniline analogue, 2,6-pyridine)

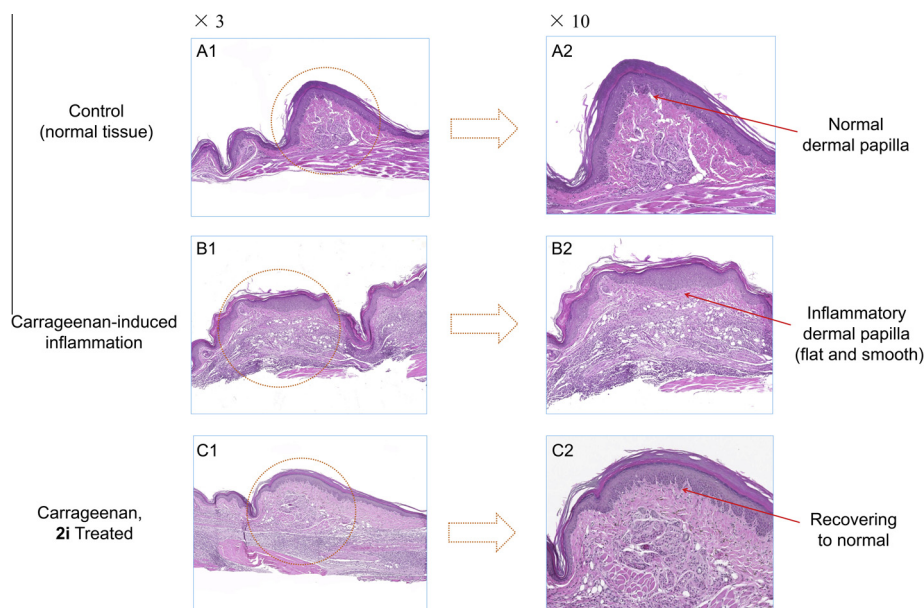


Figure 3. Histological assay of compound **2i**. Paw tissue sections were stained with H&E. The whole tissue slices were scanned/digitized by NanoZoomer 2.0 HT. Software NDP.view 2 was used to zoom in.

Table 3
Docking scores and key residue interactions of select hit compounds

Active compound	EC (nM)	Key residue interactions
2e	1	ASP97 ^a , TRP94 ^a
2g	1	ASP97 ^a , TRP102 ^a
2i	10	ASP97 ^{a,b}
2s	1	ASP97 ^a , TRP94 ^a , TYR116 ^a , HIS113
2w	10	ASP97 ^a , ARG188 ^a , TYR116 ^a , HIS113
9c	1	ASP97 ^a , CYS186 ^a , TRP102 ^a , SER285

^a CXCL12 signaling and transduction important residue.

^b **2i** has 3 different interactions with ASP97.

and **2w** (morpholino analogue, 2,6-pyridine) suppressed inflammation by 42% and 39% respectively, which is similar to WZ811's inflammation suppression (40%). None of the other compounds reduced inflammation by more than 21%. It is interesting that several of these compounds that did not reduce the inflammation as strongly as **2g** and **2w** still showed favorable inhibition assay results. This might suggest, that although these compounds are active in cell assays, these compounds may have pharmacokinetic issues when tested in vivo.

Figure 3 shows the histological analysis of the mouse paw after completion of the study. Compared to the normal tissue (A1-2), carrageenan-induced skin inflammation exhibited intense dermal papillae edema, and a dense infiltration of inflammatory cells (B1-2). After being treated with **2i**, the edema volume decreased observably (C1-2).

2.5. Docking studies

In silico methods were utilized in order to gain further insight into the binding characteristics of the prepared ligands. Studies

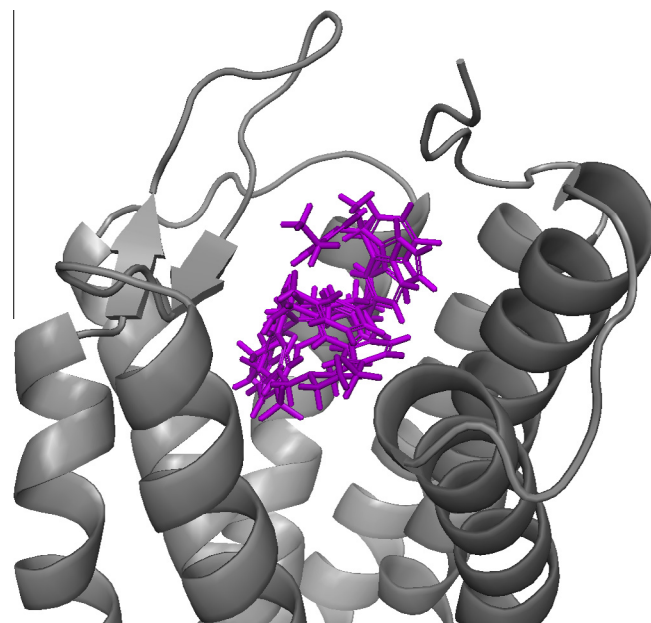


Figure 5. Superimposition of the active compounds show the compounds occupy a common region of the active site.

have found several key residues required for CXCL12 binding including ASP97, GLU288, ASP187, PHE87, ASP171, and PHE292, while the first three are required for CXCL12 signaling.^{28,29} All the active pyridine analogues share a common polar interaction with CXCR4/CXCL12 binding and signaling residue ASP97, while most have interactions with other notable residues such as

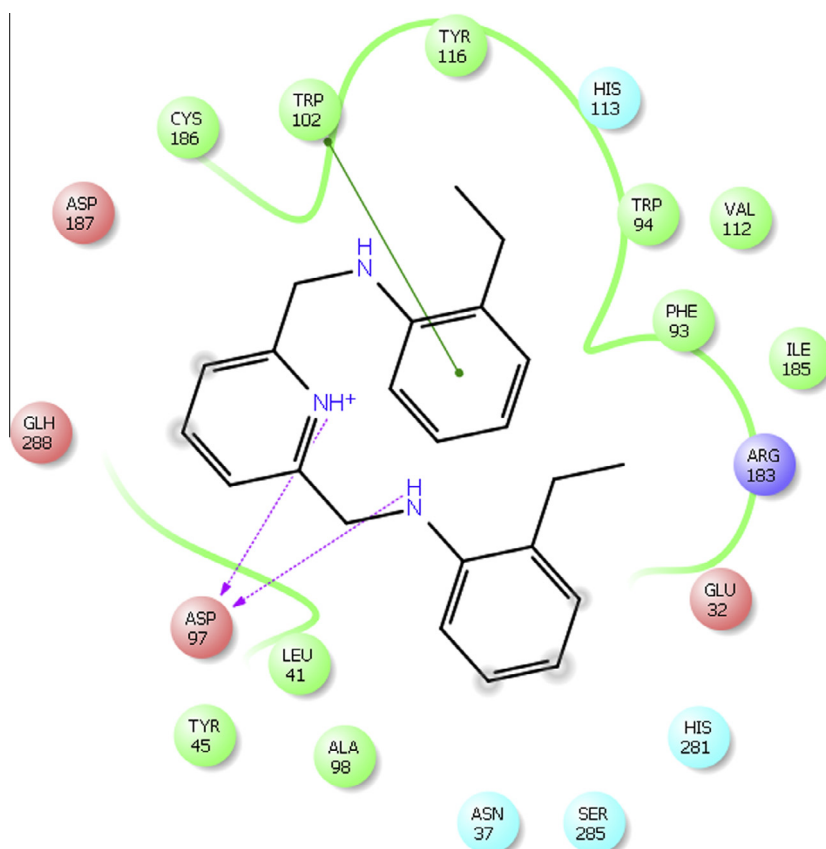


Figure 4. Active analog **2e** CXCR4 interactions with ASP97 and TRP102.

CYS186, TRP102, TRP94, and TYR116 (Table 3). Active analog **2e** has a protonated pyridine ring and has one of the better docking scores of -6.594 kcal/mol (Fig. 4). Compound **2e** shows polar and pi–pi interactions with important CXCR4/CXCL12 binding residues ASP97 and TRP102. Superimposition of all the active analogs shows that all the potent compounds occupy a common area of the active site (Fig. 5). The inactive compounds do not share any interactions with these important residues.

These *in silico* results have shown that all active compounds share interactions with residues, which play key roles with CXCL12 signaling and transduction. Docking results revealed that all potent analogs share polar interactions with key residue ASP 97, while some showed interactions with other CXCR4/CXCL12 binding residues CYS186, TRP102, TRP94, and TYR116.

3. Conclusions

Several new promising antagonistic CXCR4 analogues were synthesized and tested for activity. Nine hit compounds were identified from the preliminary assays with an EC of 100 nm in the binding assay and invasion inhibition above 35%. These hit compounds were subjected to the carrageenan paw inflammation test where two of the compounds (**2g** and **2w**) reduced inflammation on par with WZ811, which reduced inflammation by 40%. These two compounds were further analyzed using the binding assay described earlier, to obtain IC₅₀ values. **2g** and **2w** showed an IC₅₀ of 19.6 nM and 35.7 nM respectively. These results demonstrate both the utility of the binding assay as a preliminary screen and the potency of these compounds as CXCR4 antagonists.

The potency of the 2,6-pyridine compounds was further probed using docking studies. The docking results suggest that compounds that interact with ASP97 have a stronger inhibition of CXCR4. These results have provided a foundation in which to expand for future work in creating more heterocyclic-based antagonists. Future directions for this work will include expanding the 2,5 pyridine libraries as well as the incorporation of other heterocyclic aromatic ring based scaffolding. These future syntheses will also include a broader spectrum of amino-based R-groups including aromatic compounds and heterocyclic rings such as piperazine as well as benzyl amine derivatives to increase the length of the compounds. Additional tests in future studies would include probes for specificity and a probe into the pharmacokinetic properties of the analogues.

4. Experimental

4.1. Chemistry

The ¹H NMR (400 MHz) and ¹³C NMR (100 MHz) spectra were recorded on a Bruker Ac 400 FT NMR spectrometer in deuterated chloroform (CDCl₃). All chemical shifts were reported using parts per million (ppm). Mass spectra were recorded on a JEOL spectrometer at Georgia State University Mass Spectrometry Center.

4.1.1. General procedure for the synthesis of the 2,6-pyridine analogs (**2**)

To a solution of pyridine-2,6-dicarbaldehyde (50 mg, 0.37 mmol) in methanol (2 mL) was added the aniline derivative of choice (0.81 mmol) and ZnCl₂ (100 mg, 0.74 mmol). The solution was stirred for two hours at room temperature. NaBH₃CN (46.5 mg, 0.81 mmol) was then added and the solution as stirred overnight. The crude product was purified by column chromatography.

4.1.1.1. 2,6-Bis(anilinomethyl)pyridine, (2a). Product was obtained in 37% yield as an off-white semi-solid. ¹H NMR (399.99 MHz, CDCl₃): δ ppm 4.38 (s, 4H), 6.59 (d, *J* = 7.8 Hz, 4H), 6.65 (t, *J* = 7.2 Hz, 2H), 7.06–7.15 (m, 6H), 7.49 (t, *J* = 7.7 Hz, 1H);

¹³C NMR (399.9 MHz, CDCl₃): δ ppm 158.1, 148.0, 137.3, 129.3, 119.9, 117.7, 113.1, 49.3; HRMS: *m/z* [M+H]⁺ calcd for C₁₉H₁₉N₃: 290.1657, found: 290.1657.

4.1.1.2. 2,6-Bis(2-methylanilinomethyl)pyridine, (2b). The product obtained was an orange oil in 21% yield. ¹H NMR (399.99 MHz, CDCl₃): δ ppm 2.25 (s, 6H), 4.52 (s, 4H), 6.60 (d, *J* = 7.83 Hz, 2H), 6.68 (t, *J* = 7.33 Hz, 2H), 7.05–7.14 (m, 4H), 7.22 (d, *J* = 7.83 Hz, 2H), 7.60 (t, *J* = 7.71 Hz, 1H); ¹³C NMR (399.9 MHz, CDCl₃): δ ppm 158.02, 145.84, 137.26, 130.08, 127.13, 122.27, 119.99, 117.22, 110.14, 49.22, 17.59; HRMS: *m/z* [M+H]⁺ calcd for C₂₁H₂₃N₃: 318.1965, found: 318.1958.

4.1.1.3. 2,6-Bis(3-methylanilinomethyl)pyridine, (2c). The product obtained was an orange oil in 50% yield. ¹H NMR (399.99 MHz, CDCl₃): δ ppm 2.26 (s, 6H) 4.42 (s, 4H) 6.42–6.52 (m, 4H) 6.54 (d, *J* = 7.33 Hz, 2H) 7.06 (t, *J* = 7.58 Hz, 2H) 7.17 (d, *J* = 7.58 Hz, 2H) 7.54 (t, *J* = 7.58 Hz, 1H); ¹³C NMR (399.9 MHz, CDCl₃): δ ppm 158.23, 148.06, 139.06, 137.26, 129.20, 119.86, 118.61, 113.95, 110.23, 49.30, 21.70. HRMS: *m/z* [M+Z]⁺ calcd for C₂₁H₂₃N₃: 318.1965, found: 318.1965.

4.1.1.4. 2,6-Bis(4-methylanilinomethyl)pyridine, (2d). The product obtained was a yellow-orange solid in 34% yield. ¹H NMR (399.99 MHz, CDCl₃): δ ppm 2.24 (s, 6H) 4.43 (s, 4H) 6.59 (d, *J* = 8.34 Hz, 4H) 6.99 (d, *J* = 8.08 Hz, 4H) 7.19 (d, *J* = 7.83 Hz, 2H) 7.56 (t, *J* = 7.71 Hz, 1H); ¹³C NMR (399.9 MHz, CDCl₃): δ ppm 158.36, 145.70, 137.22, 129.78, 126.84, 119.85, 113.27, 49.64, 20.42. HRMS: *m/z* [M+Z]⁺ calcd for C₂₁H₂₃N₃: 318.1965, found: 318.1962.

4.1.1.5. 2,6-Bis(2-ethylanilinomethyl)pyridine, (2e). The product was obtained in 53% yield as a brown solid. ¹H NMR (399.99 MHz, CDCl₃): δ ppm 1.31 (t, *J* = 7.45 Hz, 6H), 2.60 (q, *J* = 7.58 Hz, 4H), 4.52 (s, 4H), 6.61 (d, *J* = 7.83 Hz, 2H), 6.73 (t, *J* = 7.33 Hz, 2H), 7.06–7.14 (m, 4H), 7.18–7.25 (m, 2H), 7.58 (t, *J* = 7.71 Hz, 1H); ¹³C NMR (399.9 MHz, CDCl₃): δ ppm 158.17, 145.32, 137.29, 127.89, 127.04, 119.98, 117.43, 110.50, 49.36, 23.98, 12.92. HRMS: *m/z* [M+H]⁺ calcd for C₂₃H₂₇N₃: 346.2278, found: 346.2276.

4.1.1.6. 2,6-Bis(3-ethylanilinomethyl)pyridine, (2f). The product obtained was an orange oil in 23% yield. ¹H NMR (399.99 MHz, CDCl₃): δ ppm 1.18–1.24 (m, 6H), 2.56 (d, *J* = 6.32 Hz, 4H), 4.46 (br s, 4H), 6.52 (d, *J* = 14.65 Hz, 4H), 6.59 (br s, 2H), 7.02–7.15 (m, 2H), 7.21 (d, *J* = 4.04 Hz, 2H), 7.51–7.62 (m, 1H); ¹³C NMR (399.9 MHz, CDCl₃): δ ppm 158.15, 148.10, 145.45, 137.20, 129.19, 119.83, 117.36, 112.80, 110.34, 49.31, 29.02, 15.57; HRMS: *m/z* [M+H]⁺ calcd for C₂₃H₂₇N₃: 346.2278, found: 346.2285.

4.1.1.7. 2,6-Bis(4-ethylanilinomethyl)pyridine, (2g). The product obtained in 11% yield as an orange oil; ¹H NMR (399.99 MHz, CDCl₃): δ ppm 1.18 (t, *J* = 7.6 Hz, 6H), 2.50–2.57 (m, 4H), 4.41 (s, 4H), 6.59 (d, *J* = 8.3 Hz, 4H), 6.97 (d, *J* = 8.1 Hz, 2H), 7.01 (d, *J* = 8.3 Hz, 4H), 7.53 (t, *J* = 7.7 Hz, 1H); ¹³C NMR (399.9 MHz, CDCl₃): δ ppm 158.4, 146.0, 137.3, 133.6, 128.7, 119.9, 115.3, 113.3, 49.7, 28.0, 16.02. HRMS: *m/z* [M+H]⁺ calcd for C₂₃H₂₇N₃: 346.2283, found: 346.2291.

4.1.1.8. 2,6-Bis(2-fluoroanilinomethyl)pyridine, (2h). The product was obtained in 7% yield as an orange oil. ¹H NMR (399.99 MHz, CDCl₃): δ ppm 4.51 (br s, 4H), 6.59–6.74 (m, 4H), 6.88–7.07 (m, 4H), 7.24 (d, *J* = 5.05 Hz, 2H), 7.61 (d, *J* = 6.06 Hz, 1H); ¹³C NMR (399.9 MHz, CDCl₃): δ ppm 157.81, 152.93, 137.39, 136.33, 124.56, 119.85, 116.96, 114.57, 112.50, 48.90; HRMS: *m/z* [M+H]⁺ calcd for C₁₉H₁₇N₃F₂: 326.1463, found: 326.1451.

4.1.1.9. 2,6-Bis(3-fluoroanilinomethyl)pyridine, (2i). Product was obtained in 62% yield as a brown semi-solid. ^1H NMR (399.99 MHz, CDCl_3): δ ppm 4.34 (s, 4H), 6.21–6.40 (m, 6H), 6.95–7.06 (m, 2H), 7.10 (d, $J = 7.8$ Hz, 2H), 7.51 (t, $J = 7.71$ Hz, 1H); ^{13}C NMR (399.9 MHz, CDCl_3): δ ppm 165.4, 162.9, 157.5, 149.8, 149.7, 137.4, 130.3120.1, 109.0, 104.2, 104.0, 99.9, 99.6, 48.9; HRMS: m/z $[\text{M}+\text{H}]^+$ calcd for $\text{C}_{19}\text{H}_{17}\text{N}_3\text{F}_2$: 326.1469, found: 326.1462.

4.1.1.10. 2,6-Bis(4-fluoroanilinomethyl)pyridine, (2j). Product was obtained in 34% yield as a brown semi-solid; ^1H NMR (399.99 MHz, CDCl_3): δ ppm 4.33 (s, 4H), 6.51 (dd, $J = 8.72$, 4.17 Hz, 4H), 6.81 (t, $J = 8.59$ Hz, 4H), 7.12 (d, $J = 7.58$ Hz, 2H), 7.52 (t, $J = 7.71$ Hz, 1H); ^{13}C NMR (399.9 MHz, CDCl_3): δ ppm 158.0, 157.2, 154.8, 137.4, 137.2, 120.0, 115.9, 115.7, 115.6, 115.5, 114.3, 113.5, 113.4, 49.9; HRMS: m/z $[\text{M}+\text{H}]^+$ calcd for $\text{C}_{19}\text{H}_{17}\text{N}_3\text{F}_2$: 326.1469, found: 326.1462.

4.1.1.11. 2,6-Bis(2-chloroanilinomethyl)pyridine, (2k). The product was obtained in 39% yield as a yellow solid. ^1H NMR (399.99 MHz, CDCl_3): δ ppm 4.54 (d, $J = 5.05$ Hz, 4H), 6.61–6.69 (m, 4H), 7.10 (t, $J = 7.45$ Hz, 2H), 7.21 (d, $J = 7.58$ Hz, 2H), 7.28 (d, $J = 7.58$ Hz, 2H), 7.61 (t, $J = 7.71$ Hz, 1H); ^{13}C NMR (399.9 MHz, CDCl_3): δ ppm 157.64, 143.70, 137.42, 139.18, 137.80, 119.83, 119.49, 117.45, 111.63, 48.94. HRMS: m/z $[\text{M}+\text{H}]^+$ calcd for $\text{C}_{19}\text{H}_{17}\text{N}_3\text{Cl}_2$: 358.0872, found: 358.0877.

4.1.1.12. 2,6-Bis(3-chloroanilinomethyl)pyridine, (2l). Product was obtained in 14% yield as a yellow semi-solid; ^1H NMR (399.99 MHz, CDCl_3): δ ppm 4.36 (s, 4H), 6.46 (dd, $J = 8.1$, 1.0 Hz, 2H), 6.58 (s, 2H), 6.61 (d, $J = 7.8$ Hz, 2H), 7.01 (t, $J = 8.0$ Hz, 2H), 7.12 (d, $J = 7.6$ Hz, 2H), 7.54 (t, $J = 7.71$ Hz, 1H); ^{13}C NMR (399.9 MHz, CDCl_3): δ ppm 157.4, 149.0, 137.5, 135.1, 130.3, 120.1, 117.5, 112.7, 111.4, 48.9. HRMS: m/z $[\text{M}+\text{H}]^+$ calcd for $\text{C}_{19}\text{H}_{17}\text{N}_3\text{Cl}_2$: 358.0854, found: 358.0864.

4.1.1.13. 2,6-Bis(4-chloroanilinomethyl)pyridine, (2m). Product obtained in 15% yield as a yellow solid; mp 116–118 °C. ^1H NMR (399.99 MHz, CDCl_3): δ ppm 4.36 (br s, 4H), 6.51 (d, $J = 8.34$ Hz, 4H), 7.06 (d, $J = 8.34$ Hz, 4H), 7.12 (d, $J = 7.6$ Hz, 2H), 7.54 (t, $J = 7.7$ Hz, 1H); ^{13}C NMR (399.9 MHz, CDCl_3): δ ppm 157.6, 146.4, 137.4, 129.1, 122.3, 120.0, 114.2, 49.2. HRMS: m/z $[\text{M}+\text{H}]^+$ calcd for $\text{C}_{19}\text{H}_{17}\text{N}_3\text{Cl}_2$: 358.0872, found: 358.0864.

4.1.1.14. 2,6-Bis(2-methoxyanilinomethyl)pyridine, (2n). The product obtained in 51% yield as a brown solid; mp 112–114 °C. ^1H NMR (399.99 MHz, CDCl_3): δ ppm 3.81 (s, 6H), 4.43 (s, 4H), 6.49 (d, $J = 7.58$ Hz, 2H), 6.58–6.64 (m, 2H), 6.70–6.79 (m, 4H), 7.14 (d, $J = 7.8$ Hz, 2H), 7.48 (t, $J = 7.7$ Hz, 1H); ^{13}C NMR (399.9 MHz, CDCl_3): δ ppm 158.7, 147.0, 137.9, 137.3, 121.3, 119.6, 116.7, 110.3, 109.5, 55.5, 49.4. HRMS: m/z $[\text{M}+\text{H}]^+$ calcd for $\text{C}_{21}\text{H}_{23}\text{N}_3\text{O}_2$: 350.1869, found: 350.1862.

4.1.1.15. 2,6-Bis(3-methoxyanilinomethyl)pyridine, (2o). The product was obtained in 16% yield as an off white semisolid. ^1H NMR (399.99 MHz, CDCl_3): δ ppm 3.76 (br s, 6H), 4.45 (br s, 4H), 6.23 (br s, 2H), 6.30 (m, 4H), 7.09 (d, $J = 3.28$ Hz, 2H), 7.20 (m, 2H), 7.59 (m, 1H); ^{13}C NMR (399.9 MHz, CDCl_3): δ ppm 160.79, 157.91, 149.30, 137.28, 130.00, 119.89, 106.18, 102.75, 99.03, 55.08, 49.19; HRMS: m/z $[\text{M}+\text{H}]^+$ calcd for $\text{C}_{21}\text{H}_{23}\text{N}_3\text{O}_2$: 350.1863, found: 350.1854.

4.1.1.16. 2,6-Bis(4-methoxyanilinomethyl)pyridine, (2p). Product obtained in 30% yield as a brown solid; mp 63–65 °C. ^1H NMR (399.99 MHz, CDCl_3): δ ppm 3.66 (s, 6H), 4.33 (s, 4H), 6.55 (d, $J = 8.84$ Hz, 4H), 6.70 (d, $J = 8.84$ Hz, 4H), 7.12 (d, $J = 7.58$ Hz,

2H), 7.49 (t, $J = 7.7$ Hz, 1H); ^{13}C NMR (399.9 MHz, CDCl_3): δ ppm 158.39, 152.25, 142.22, 137.20, 119.94, 114.90, 114.36, 55.79, 50.24; HRMS: m/z $[\text{M}+\text{H}]^+$ calcd for $\text{C}_{21}\text{H}_{23}\text{N}_3\text{O}_2$: 350.1869, found: 350.1865.

4.1.1.17. 2,6-Bis(2-trifluoromethylanilinomethyl)pyridine, (2q). The product was obtained in 19% yield as an off white solid. ^1H NMR (399.99 MHz, CDCl_3): δ ppm 4.55 (d, $J = 5.05$ Hz, 4H), 6.63–6.79 (m, 4H), 7.20 (d, $J = 7.58$ Hz, 2H), 7.32 (t, $J = 7.71$ Hz, 2H), 7.47 (d, $J = 7.58$ Hz, 2H), 7.61 (t, $J = 7.71$ Hz, 1H); ^{13}C NMR (399.9 MHz, CDCl_3): δ ppm 157.32, 145.14, 137.58, 133.14, 126.72, 126.67, 119.77, 116.27, 113.66, 112.26, 48.69. HRMS: m/z $[\text{M}+\text{H}]^+$ calcd for $\text{C}_{21}\text{H}_{17}\text{F}_6\text{N}_3$: 426.1401, found: 426.1399.

4.1.1.18. 2,6-Bis(3-trifluoromethylanilinomethyl)pyridine, (2r). The product obtained in 50% yield as an off white solid. ^1H NMR (399.99 MHz, CDCl_3): δ ppm 4.46 (br s, 4H) 6.78 (d, $J = 8.08$ Hz, 2H) 6.87 (br s, 2H) 6.95 (d, $J = 7.58$ Hz, 2H) 7.19 (d, $J = 7.83$ Hz, 2H) 7.25 (t, $J = 1.00$ Hz, 2H) 7.61 (t, $J = 7.71$ Hz, 1H); ^{13}C NMR (399.9 MHz, CDCl_3): δ ppm 157.24, 148.06, 137.51, 131.75, 129.71, 125.74, 123.03, 120.20, 116.02, 114.05, 109.23, 48.80. HRMS: m/z $[\text{M}+\text{H}]^+$ calcd for $\text{C}_{21}\text{H}_{17}\text{F}_6\text{N}_3$: 426.1399, found: 426.1384.

4.1.1.19. 2,6-Bis(4-trifluoromethylanilinomethyl)pyridine, (2s). The product obtained in 61% yield as a light orange semi-solid. ^1H NMR (399.99 MHz, CDCl_3): δ ppm 4.49 (s, 4H) 6.65 (d, $J = 8.34$ Hz, 4H) 7.20 (d, $J = 7.83$ Hz, 2H) 7.41 (d, $J = 8.34$ Hz, 4H) 7.63 (t, $J = 1.00$ Hz, 1H); ^{13}C NMR (399.9 MHz, CDCl_3): δ ppm 157.15, 150.28, 137.59, 126.68, 126.32, 123.64, 120.15, 112.21, 48.46. HRMS: m/z $[\text{M}+\text{H}]^+$ calcd for $\text{C}_{21}\text{H}_{17}\text{F}_6\text{N}_3$: 426.1399, found: 426.1381.

4.1.1.20. 2,6-Bis(4-thiomethylanilinomethyl)pyridine, (2t). The product obtained in 14% yield as a white solid; ^1H NMR (399.99 MHz, CDCl_3): δ ppm 2.41 (s, 6H) 4.44 (br s, 4H) 6.61 (d, $J = 8.34$ Hz, 4H) 7.16–7.31 (m, 6H) 7.59 (t, $J = 7.71$ Hz, 1H); ^{13}C NMR (399.9 MHz, CDCl_3): δ ppm 19.02, 49.12, 113.70, 119.94, 124.61, 131.34, 137.30, 146.70, 157.80. HRMS: m/z $[\text{M}+\text{H}]^+$ calcd for $\text{C}_{21}\text{H}_{24}\text{N}_3\text{S}_2$: 382.1206, found: 382.1404.

4.1.1.21. 2,6-Bis(3-nitroanilinomethyl)pyridine, (2u). The product obtained in 34% yield as a yellow-orange solid; mp 147–149 °C. ^1H NMR (399.99 MHz, CDCl_3): δ ppm 4.54 (d, $J = 5.05$ Hz, 4H), 6.96 (d, $J = 8.08$ Hz, 2H), 7.24 (br s, 2H), 7.31 (t, $J = 8.1$ Hz, 2H), 7.49 (br s, 2H), 7.56 (d, $J = 8.08$ Hz, 2H), 7.65–7.71 (m, 1H); ^{13}C NMR (399.9 MHz, CDCl_3): δ ppm 156.8, 148.6, 137.7, 129.8, 120.4, 119.2, 112.4, 106.6, 48.7. HRMS: m/z $[\text{M}+\text{H}]^+$ calcd for $\text{C}_{19}\text{H}_{17}\text{N}_5\text{O}_4$: 380.1359, found: 380.1358.

4.1.1.22. 2,6-Bis(4-nitroanilinomethyl)pyridine, (2v). The product obtained in 10% yield as a yellow semi-solid; ^1H NMR (399.99 MHz, CDCl_3): δ ppm 4.51 (d, $J = 5.1$ Hz, 4H), 6.56 (d, $J = 9.1$ Hz, 4H), 7.17 (d, $J = 7.8$ Hz, 2H), 7.64 (t, $J = 7.71$ Hz, 1H), 8.05 (d, $J = 9.09$ Hz, 2H); ^{13}C NMR (399.9 MHz, CDCl_3): δ ppm 156.1, 152.7, 137.9, 126.4, 120.5, 111.6, 48.9. HRMS: m/z $[\text{M}+\text{H}]^+$ calcd for $\text{C}_{19}\text{H}_{18}\text{N}_5\text{O}_4$: 380.1359, found: 380.1359.

4.1.1.23. 2,6-Bis(morpholinylmethyl)pyridine (2w). The product obtained was a white semi-solid in 1% yield. ^1H NMR (399.99 MHz, CDCl_3): δ ppm 7.73 (1H t), 7.47 (2H d), 5.30 (4H s), 2.60 (8H m), 1.65 (8H m), 1.50 (4H, m); ^{13}C NMR (399.9 MHz, CDCl_3): δ ppm 152.75, 137.55, 123.65, 120.96, 60.43, 63.80, 25.68, 25.11, 23.78. HRMS: m/z $[\text{M}+\text{H}]^+$ calcd for $\text{C}_{15}\text{H}_{23}\text{N}_3\text{O}_2$: 278.1863, found: 278.1852.

4.1.2. General procedure for the preparation of 2,5-diamino dicarbaldehyde pyridine analogs

To a stirred solution 2,5-diaminopyridine (1.3 equiv) in anhydrous MeOH were added a benzaldehyde (2.0 equiv), and dried ZnCl₂ (3.0 equiv). Sodium cyanoborohydride (3 equiv) in anhydrous MeOH was added to the reaction mixture. The reaction was allowed to stir at room temperature for 1–2 h and progress followed by TLC. The solvent was evaporated off under reduced pressure. The reaction mixture was quenched with distilled water and extracted with ethyl acetate. The organic layer was dried over MgSO₄, filtered and concentrated under reduced pressure. Crude products were purified by column chromatography on silica gel to afford products.

4.1.2.1. N₂,N₅-Bis(4-methoxybenzyl)pyridine-2,5-diamine (5a). The product was obtained in 24% yield. ¹H NMR (399.99 MHz, CDCl₃): δ ppm 7.63 (s, 1H), 7.19–7.28 (m, 8H), 6.83 (dd, *J* = 8.34, 13.14 Hz, 2H), 4.29 (s, 2H), 4.12 (s, 2H), 3.78 (s, 3H), 3.76 (s, 3H). HRMS: *m/z* [M+H]⁺ calcd for C₂₁H₂₄O₂N₃: 350.1863, found: 350.1851.

4.1.2.2. N₂,N₅-Bis(4-ethoxybenzyl)pyridine-2,5-diamine (5b). The product was obtained in 3% yield. ¹H NMR (399.99 MHz, CDCl₃): δ ppm 7.36 (s, 1H), 7.25 (m, *J* = 11.87 Hz, 8H), 6.82–6.88 (m, 4H), 4.37 (s, 1H), 4.14 (s, 1H), 3.97–4.05 (m, 4H), 1.37–1.44 (m, 6H); HRMS: *m/z* [M+H]⁺ calcd for C₂₃H₂₈O₂N₃: 378.2176, found: 378.2162.

4.1.2.3. N₂,N₅-Bis(3-chlorobenzyl)pyridine-2,5-diamine (5c). The product was obtained in 37% yield. ¹H NMR (399.99 MHz, CDCl₃): δ ppm 7.60 (s, 1H), 7.34 (d, *J* = 6.82 Hz, 2H), 7.18–7.28 (m, 8H), 6.86 (d, *J* = 2.78 Hz, 1H), 6.84 (d, *J* = 2.78 Hz, 1H), 4.40 (s, 2H), 4.22 (s, 2H); HRMS: *m/z* [M+H]⁺ calcd for C₁₇H₁₈Cl₂N₃: 358.0878, found: 358.0884 (M+1).

4.1.2.4. N₂,N₅-Bis(4-fluorobenzyl)pyridine-2,5-diamine (5d). The product was obtained in 31% yield. ¹H NMR (399.99 MHz, CDCl₃): δ ppm 7.44 (s, 1H), 7.00 (d, *J* = 7.33 Hz, 8H), 6.39–6.42 (m, 1H) 6.37–6.40 (m, 1H), 4.34 (s, 2H), 4.20 (s, 2H); HRMS: *m/z* [M+H]⁺ calcd for C₁₉H₁₈F₂N₃: 326.1469, found: 326.147.

4.1.3. 2,5-Dicarbaldehyde pyridine synthesis pyridine-2,5-diyl dimethanol (7)

2,5-Dimethyl carboxylate pyridine (1 equiv) in EtOH was cooled to 0 °C. Sodium borohydride (7 equiv) was added to the cooled 0 °C reaction mixture. The reaction mixture was stirred for 1 h at 0 °C, 3 h at rt, and refluxed for 12 h and progress followed by TLC. The reaction was quenched with distilled water. The reaction mixture was then centrifuged and the supernatant was poured off. Silica gel was then added to the supernatant liquid and concentrated under reduced pressure. The silica gel and crude solid was purified by column chromatography (20:1 DCM/MeOH) to afford the 2,5-dimethanol pyridine. Product was obtained in 51% yield. HRMS: *m/z* [M+H]⁺ calcd for C₇H₁₀O₂N: 140.0706, found: 140.0703.

4.1.4. Pyridine-2,5-dicarbaldehyde (8)

To a stirred solution 2,5-dimethanol pyridine (1 equiv) in anhydrous 1,4-dioxane (0.14 M) was added dried activated MnO₂ (5 equiv). The reaction mixture was stirred at 96 °C under reflux under nitrogen for 1 h and progress followed by TLC. The reaction was cooled, quenched with distilled water, filtered, and concentrated under reduced pressure. Crude products were purified by column chromatography (4:1 Hexane/Ethyl acetate) on silica gel to afford 2,5-dicarbaldehyde pyridine. Product was obtained in

53% yield. ¹H NMR (399.99 MHz, CDCl₃): δ ppm 10.24 (s, 1H), 10.18 (s, 1H), 9.26 (s, 1H), 8.36 (d, *J* = 10.10 Hz, 1H), 8.13 (d, *J* = 10.10 Hz, 1H). ¹³C NMR (399.9 MHz, CDCl₃): δ ppm 121.45, 133.25, 137.0, 151.59, 155.32, 189.56, 192.05.

4.1.5. General procedure for the preparation of 2,5-dicarbaldehyde pyridine analogs (9a–9c)

To a stirred solution pyridine-2,5-dicarbaldehyde (1.0 equiv) in 1,2-dichloroethane (0.27 M) were added an aniline (2.2 equiv), and sodium triacetoxyborohydride (3.0 equiv). Acetic acid (2.0 equiv) was added after five minutes. The reaction was allowed to stir at room temperature for 5 h and progress followed by TLC. The reaction mixture was quenched with NaOH and extracted with ethyl acetate. The organic layer was dried over MgSO₄, filtered and concentrated under reduced pressure. Crude products were purified by column chromatography on silica gel to afford products.

4.1.5.1. N,N'-(Pyridine-2,5-diylbis(methylene))bis(4-ethylani-line) (9a). Product was obtained in 8% yield. ¹H NMR (399.99 MHz, CDCl₃): δ ppm 8.56–8.59 (m, 1H), 7.62–7.67 (m, 2H), 7.37–7.41 (m, 2H), 7.29–7.33 (m, 2H), 6.59 (dd, *J* = 8.34, 13.64 Hz, 4H), 4.43 (s, 1H), 4.32 (s, 1H), 2.54 (q, *J* = 7.60 Hz, 4H), 1.14–1.27 (m, 6H); HRMS: *m/z* [M+H]⁺ calcd for C₂₃H₂₈N₃: 346.2283, found: 346.2287.

4.1.5.2. N,N'-(Pyridine-2,5-diylbis(methylene))bis(3-fluoroani-line) (9b). Product was obtained in 13% yield. ¹H NMR (399.99 MHz, CDCl₃): δ ppm 8.58 (br s, 1H), 7.58–7.72 (m, 1H), 7.28 (d, *J* = 9.09 Hz, 1H), 7.03–7.14 (m, 2H), 6.25–6.46 (m, 6H), 4.43 (br s, 2H), 4.33 (br s, 2H); HRMS: *m/z* [M+H]⁺ calcd for C₁₉H₁₈F₂N₃: 326.1463, found: 326.1453.

4.1.5.3. N,N'-(Pyridine-2,5-diylbis(methylene))bis(3-methylani-line) (9c). Product was obtained in 8% yield. ¹H NMR (399.99 MHz, CDCl₃): δ ppm 8.58 (s, 1H), 7.06 (t, *J* = 7.58 Hz, 1H), 6.56 (t, *J* = 7.83 Hz, 1H), 6.41–6.51 (m, 6H), 4.44 (s, 2H), 4.33 (s, 2H), 2.27 (s, 6H); HRMS: *m/z* [M+H]⁺ calcd for C₂₁H₂₄N₃: 318.1965, found: 318.1965.

4.2. Primary binding affinity screening

The binding affinity assay is a competitive assay where twenty thousand MDA-MB-231 breast cancer cells are incubated in an 8-well slide chamber for two days in 300 μL of medium. The compounds were also incubated in separate wells at several concentrations (1, 10, 100, 1000 nM) for ten minutes at room temperature. The cells were then fixed in a chilled solution of 4% paraformaldehyde. After the cells were rehydrated in phosphate-buffered saline (PBS), the slides were prepared by incubating them with 0.05 μg/mL biotinylated **TN14003** for thirty minutes at room temperature. These slides were washed three times with the PBS solution and were then incubated for thirty minutes at room temperature in streptavidin–rhodamine (1:150 dilution; Jackson ImmunoResearch Laboratories, West Grove, PA). The slides were washed again with the PBS solution and were mounted in an antifade mounting solution (Molecular Probes, Eugene, OR). A Nikon Eclipse E800 microscope was used to analyze the samples.^{22,30}

4.3. Matrigel invasion assay

This assay was performed using a Matrigel invasion chamber (Corning Biocoat; Bedford, MA). In the bottom chamber, a solution of CXCL12 (200 ng/mL; R&D Systems, Minneapolis, MN) was added to the apparatus. 100 nm of the selected compounds (or AMD3100 as a control) were added to the MDA-MB-231. The cells were then

placed in the top chamber. The apparatus was then incubated in a humidified incubator for 22 h. The remaining cells in the top chamber were removed using a cotton swab and the invading cells in the bottom chamber were stained hematoxylin and eosin (H&E) and fixed with methanol. The rate of invasion was calculated by counting the invading (stained) cells.^{22,30}

4.4. Paw inflammation suppression test

In this test, C57BL/6J does (Jackson Laboratories) are subcutaneously injected with λ -carrageenan (50 μ L in 1% w/v in saline) in the right hind paw to trigger inflammation; the other hind paw is used as the non-inflammation control. The selected analogues were prepared in 10% DMSO and 90% of 45% (2-hydroxypropyl)- β -cyclodextrin (CD) in PBS. Doses of the analogues were set at 10 mg/kg and the dose for TN14003 was set at 300 μ g/kg. The TN14003 dose was set lower for this experiment because it was found that 300 μ g/kg gave the maximum efficacy at minimum concentration in breast cancer metastasis in an animal model. The mice were dosed 30 min after the carrageenan injection and then once a day following the initial dose. The mice were sacrificed 74 h after inflammation was induced and two hours after the last injection of the selected analogues. The hind paws of the mice were photographed and calipers were used to measure the thickness of the paw from front to back. To quantify the edema, the volume of the untreated paw was subtracted from the volume of the treated paw. The inflammation suppression percentage was determined by comparing the analogue treated groups to the control group. Each analogue was tested in quintuplicate using the above procedure.^{22,26}

Paw tissue slices were also collected and stained with H&E. Tissue slices were scanned and digitized by NanoZoomer 2.0 HT. The software NDP.view 2 was used to view the slices in detail.

4.5. Docking studies

The structure of the target receptor CXCR4, PDB-ID 3ODU, was retrieved from the RCSB Protein Data Bank.³¹ Docking calculations were performed by the Schrodinger suite with default settings unless otherwise indicated.³² The Protein Preparation Wizard was used to prepare the CXCR4 protein for docking. CXCR4 along with its co-crystallized ligand IT1t went through a preprocess procedure with the additional options to fill in missing side chains and loops using Prime and removing waters beyond 5 Å from heteroatom groups. The heterostate for the co-crystallized ligand was generated using Epik. The PROPKA feature was utilized to optimize the hydrogen bond network at a physiological pH. After hydrogen bond optimization, water molecules were removed with less than 3H-bonds to non-waters. The protein was then energetically minimized using a default constraint of 0.3 Å RMSD and OPLS 2005 force field. Ligands were prepared by the Ligprep function of the Schrodinger Suite with default parameters in the gas phase. Epik generated possible ionization states of the ligands at physiological pH. Receptor grid generation was performed by inputting the prepared receptor directly from the protein preparation wizard. Docking was performed using the Extra Precision (XP) feature of the GLIDE program. Ligands were docked flexibly in the rigid protein devoid of the IT1t ligand and were ranked based on their GLIDE docking score.

Acknowledgements

We thank the following for funding: GAANN, United States Department of Education P200A150308 (TG), Department of Chemistry, Georgia State University (SRM), NIH IRACDA K12GM084897 (DC) and NIH R01CA165306 (HS).

References and notes

1. *SEER Cancer Statistics Review, 1975–2012*; Howlader, N., Noone, A. M., Krapcho, M., Garshell, J., Miller, D., Altekruse, S. F., Kosary, C. L., Yu, M., Ruhl, J., Tatalovich, Z., Mariotto, A., Lewis, D. R., Chen, H. S., Feuer, E. J., Cronin, K. A., Eds., 2014.
2. Kohler, B. A.; Sherman, R. L.; Howlader, N.; Jemal, A.; Ryerson, A. B.; Henry, K. A.; Boscoe, F. P.; Cronin, K. A.; Lake, A.; Noone, A. M.; Henley, S. J.; Ehemann, C. R.; Anderson, R. N.; Penberthy, L. J. *Natl. Cancer Inst.* **2015**, *107*, djv048.
3. Mukherjee, D.; Zhao, J. *Am. J. Cancer Res.* **2013**, *3*, 46.
4. Kucia, M.; Ratajczak, J.; Reza, R.; Janowska-Wieczorek, A.; Ratajczak, M. Z. *Blood Cells Mol. Dis.* **2004**, *32*, 52.
5. Ma, Q.; Jones, D.; Borghesani, P. R.; Segal, R. A.; Nagasawa, T.; Kishimoto, T.; Bronson, R. T.; Springer, T. A. *Proc. Natl. Acad. Sci. U.S.A.* **1998**, *95*, 9448.
6. Muller, A.; Homey, B.; Soto, H.; Ge, N.; Catron, D.; Buchanan, M. E.; McClanahan, T.; Murphy, E.; Yuan, W.; Wagner, S. N.; Barrera, J. L.; Mohar, A.; Verastegui, E.; Zlotnik, A. *Nature* **2001**, *410*, 50.
7. Choi, W. T.; Duggineni, S.; Xu, Y.; Huang, Z.; An, J. *J. Med. Chem.* **2012**, *55*, 977.
8. Mathtys, P.; Hatse, S.; Vermeire, K.; Wuys, A.; Bridger, G.; Henson, G. W.; De Clercq, E.; Billiau, A.; Schols, D. *J. Immunol.* **2001**, *167*, 4686.
9. Huang, E. H.; Singh, B.; Cristofanilli, M.; Gelovani, J.; Wei, C.; Vincent, L.; Cook, K. R.; Lucci, A. *J. Surg. Res.* **2009**, *155*, 231.
10. Richert, M. M.; Vaidya, K. S.; Mills, C. N.; Wong, D.; Korz, W.; Hurst, D. R.; Welch, D. R. *Oncol. Rep.* **2009**, *21*, 761.
11. Kwong, J.; Kulbe, H.; Wong, D.; Chakravarty, P.; Balkwill, F. *Mol. Cancer Ther.* **2009**, *8*, 1893.
12. Horuk, R. *Cytokine Growth Factor Rev.* **2001**, *12*, 313.
13. De Clercq, E. *Nat. Rev. Drug Disc.* **2003**, *2*, 581.
14. De Clercq, E. *Biochem. Pharmacol.* **2009**, *77*, 1655.
15. Zhan, W.; Liang, Z.; Zhu, A.; Kurtkaya, S.; Shim, H.; Snyder, J. P.; Liotta, D. C. *J. Med. Chem.* **2007**, *50*, 5655.
16. Lefrançois, M.; Lefebvre, M. R.; Saint-Onge, G.; Boulais, P. E.; Lamothe, S.; Leduc, R.; Lavigne, P.; Heveker, N.; Escher, E. *ACS Med. Chem. Lett.* **2011**, *2*, 597.
17. Scozzafava, A.; Mastrolorenzo, A.; Supuran, C. T. *J. Enzyme Inhib. Med. Chem.* **2002**, *17*, 69.
18. Schwarz, M. K.; Wells, T. N. *Nat. Rev. Drug Disc.* **2002**, *1*, 347.
19. Hendrix, C. W.; Flexner, C.; MacFarland, R. T.; Giandomenico, C.; Fuchs, E. J.; Redpath, E.; Bridger, G.; Henson, G. W. *Antimicrob. Agents Chemother.* **2000**, *44*, 1667.
20. Liles, W. C.; Rodger, E.; Broxmeyer, H. E.; Dehner, C.; Badel, K.; Calandra, G.; Christensen, J.; Wood, B.; Price, T. H.; Dale, D. C. *Transfusion* **2005**, *45*, 295.
21. Hatse, S.; Princen, K.; Bridger, G.; De Clercq, E.; Schols, D. *FEBS Lett.* **2002**, *527*, 255.
22. Zhu, A.; Zhan, W.; Liang, Z.; Yoon, Y.; Yang, H.; Grossniklaus, H. E.; Xu, J.; Rojas, M.; Lockwood, M.; Snyder, J. P.; Liotta, D. C.; Shim, H. *J. Med. Chem.* **2010**, *53*, 8556.
23. Lebnath, B.; Xu, S.; Grande, F.; Garofalo, A.; Neamati, N. *Theranostics* **2013**, *3*, 47.
24. Altaf, A. A. S. A.; Gul, Z.; Rasool, N.; Badshah, A.; Lal, B.; Khan, E. *J. Drug Design Med. Chem.* **2015**, *1*, 1.
25. Hansch, C.; Leo, A.; Hoekman, D. H. *Exploring QSAR*; American Chemical Society: Washington, DC, 1995.
26. Liang, Z.; Zhan, W.; Zhu, A.; Yoon, Y.; Lin, S.; Sasaki, M.; Klapproth, J. M.; Yang, H.; Grossniklaus, H. E.; Xu, J.; Rojas, M.; Voll, R. J.; Goodman, M. M.; Arrendale, R. F.; Liu, J.; Yun, C. C.; Snyder, J. P.; Liotta, D. C.; Shim, H. *PLoS One* **2012**, *7*, e34038.
27. Bai, R.; Liang, Z.; Yoon, Y.; Liu, S.; Gaines, T.; Oum, Y.; Shi, Q.; Mooring, S. R.; Shim, H. *Eur. J. Med. Chem.* **2016**, *118*, 340.
28. Choi, W. T.; Tian, S.; Dong, C. Z.; Kumar, S.; Liu, D.; Madani, N.; An, J.; Sodroski, J. G.; Huang, Z. *J. Virol.* **2005**, *79*, 15398.
29. Brelot, A.; Heveker, N.; Montes, M.; Alizon, M. *J. Biol. Chem.* **2000**, *275*, 23736.
30. Mooring, S. R.; Liu, J.; Liang, Z.; Ahn, J.; Hong, S.; Yoon, Y.; Snyder, J. P.; Shim, H. *ChemMedChem* **2013**, *8*, 622.
31. Wu, B.; Chien, E. Y.; Mol, C. D.; Fenalti, G.; Liu, W.; Katritch, V.; Abagyan, R.; Brooun, A.; Wells, P.; Bi, F. C.; Hamel, D. J.; Kuhn, P.; Handel, T. M.; Cherezov, V.; Stevens, R. C. *Science* **2010**, *330*, 1066.
32. *Small-Molecule Drug Discovery Suite 2015-4: Glide, v.*; Schrödinger, LLC: New York, NY, 2015.